Modeling Direct Band-to-Band Tunneling using QTBM

Lidija Filipovic, Oskar Baumgartner, and Hans Kosina

Institute for Microelectronics, TU Wien

Gußhausstraße 27–29/E360 1040 Wien, Austria

Email: {lidijafilipovic|baumgartner|kosina}@iue.tuwien.ac.at

Abstract—This work focuses on modeling the tunneling mechanism in direct semiconductors. An effective barrier is extracted between the valence and conduction band, by defining the barrier as valence-like near the valence band and conduction band-like near the conduction band. The transition occurs at a point obtained by momentum matching. Computation of transition coefficient is performed using the quantum transmitting boundary method.

I. INTRODUCTION

As CMOS device miniaturization is reaching the limits of its potential, alternative techniques are being studied to find a sufficient replacement. Tunneling mechanisms have garnered significant interest recently since these devices can be designed to provide steep subthreshold swing, with great potential for ultra low power switching applications. The tunneling mechanism is complex and many factors affect the resulting current, making it a challenge to generate accurate tunneling models. This work focuses on modeling the one-dimensional tunneling current in direct semiconductors. Traditionally, the energy barrier between the valence and conduction bands is thought of as triangular [1], as shown in Fig. 1(a). This approach assumes only conduction band properties define the barrier. This oversimplifies the problem, resulting in a loss of accuracy. In this work, the energy barrier experienced by a tunneling particle is obtained from both valence and conduction bands. A portion of the barrier is obtained from valence band properties, the other from the conduction band [2], as explained by Fig. 1(b).

II. THEORY

The current density for tunneling from the valence to the conduction band is given by [1]

$$J_{v \to c} = \frac{q}{4\pi^3} \int v(k_v) T(k_v) f_v(E) \, d^3 k, \quad (1)$$

where $v(k_v)$ is the velocity of an electron with tunneling momentum k_v and $T(k_v)$ is the transmission coefficient. The velocity of an electron is defined by

$$v(k_v) = \frac{1}{\hbar} \frac{\partial E}{\partial k_v} \quad (2)$$

and, the total energy in the valence band can be re-written in terms of its three contributions,

$$E = E_{v0} - E_{v\perp} - \frac{\hbar^2 k_{vx}^2}{2m_v}. \quad (3)$$

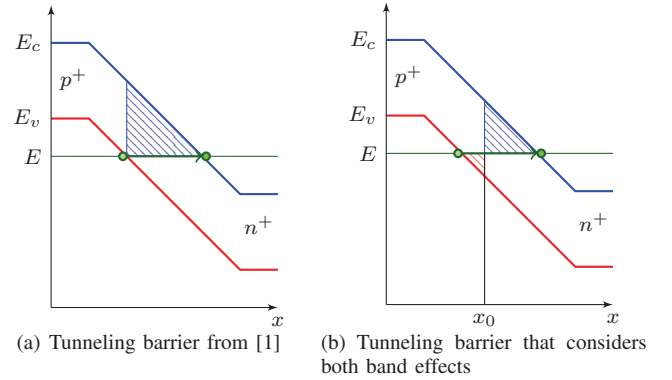(a) Tunneling barrier from [1] (b) Tunneling barrier that considers both band effects

Fig. 1. Tunneling barrier modification and the effect of transition point x_0

Eq. 1 is now partially re-written in terms of energy, in place of momentum,

$$J_{v \to c} = \frac{q}{4\hbar \pi^3} \int T(E_{v\perp}) f_v(E) \, dE_x \int d^2 k_\perp. \quad (4)$$

By assuming a 2D density of states, the integral over perpendicular wave numbers $(k_\perp)$ can be re-written as integral over perpendicular energy $(E_\perp)$ [2],

$$J_{v \to c} = \frac{q m_{v\perp}^*}{2\hbar^3 \pi^2} \int T(E_{v\perp}) f_v(E) \, dE_x \int dE_\perp. \quad (5)$$

Total current combines tunneling from valence to conduction band as well as from conduction to valence band,

$$J = J_{v \to c} - J_{c \to v}, \quad (6)$$

resulting in the overall tunneling current expression:

$$J = \frac{q m_\perp^*}{2\pi^2 \hbar^3} \int_{E_{c0}}^{E_{v0}} \int_0^{E_{\perp,max}} T(E_\perp) \, dE_\perp \left[f_v(E) - f_c(E) \right] dE \quad (7)$$

where $E_{\perp,max} = \min \left(E_{v,max} - E, E - E_{c,min} \right)$.

From this expression, we can see that the overall transmission coefficient, at an energy E, is obtained from an integral of the transmission coefficient over the perpendicular energy $E_\perp$. The tunneling barrier, at a constant energy E, increases due to the perpendicular energy contribution, $E_\perp$. This increase in barrier is demonstrated in Fig. 2. The integration over perpendicular energies can also be represented by the area under the TC curve in Fig. 3. As would be expected, the

(a) No perpendicular momentum

(b) Band diagram with tunneling path

(c) Effective tunneling energy barrier for band diagram in 2(c)

(d) Energy barrier increase due to perpendicular momentum

(e) Band diagram with tunneling path

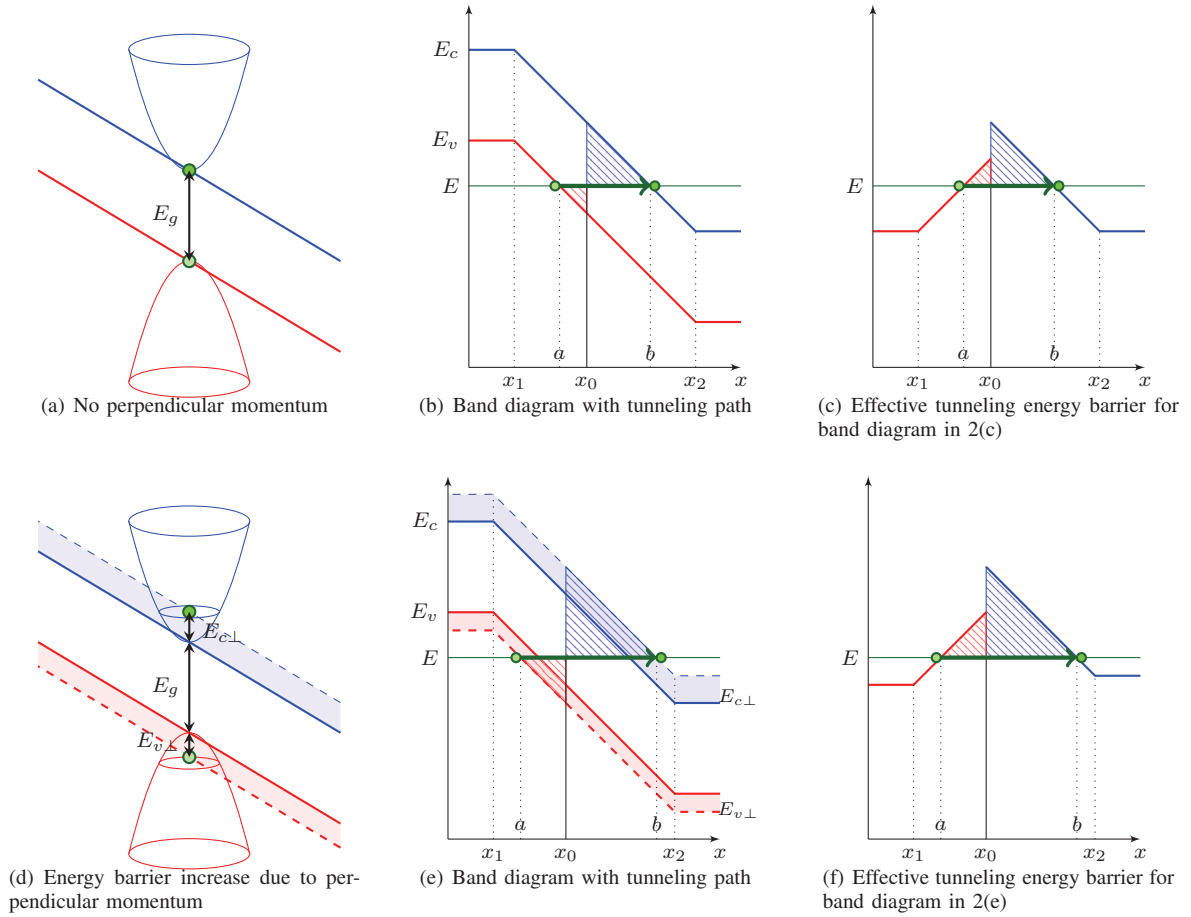(f) Effective tunneling energy barrier for band diagram in 2(e)

Fig. 2.   Tunneling barrier extraction from energy band diagram. 2(a), 2(b) and 2(c) consider no perpendicular energy contribution. Tunneling occurs at the closest point in the energy bands. 2(d), 2(e) and 2(f) show the perpendicular energy contribution.

largest transmission coefficient is obtained when $E_\perp = 0$, as this is the narrowest energy barrier of this integration. As the perpendicular energy is increased, the particle is farther away from its tunneling destination, and the effective barrier is widened, decreasing the contribution to the total transmission coefficient.

A. Parameter Extraction

In order to study the band-to-band tunneling, an energy barrier between the valence and conduction band is treated as an effective one dimensional energy barrier, Fig. 2. The negative effective mass of a particle in the valence band results in the valence band portion of the energy barrier appearing under the conduction band portion. Inverting the effective mass in the valence band, and inverting the energy band, results in the effective energy barrier from Fig. 2(c) and Fig. 2(f). The barrier has not been affected by this double inversion. It simplifies the problem to a one-dimensional tunneling potential barrier. This barrier is set to exhibit valence band properties until a transition point, and conduction band properties after this transition. Recent works have assumed a mid-way transition with some success [3], while others have used a momentum matching condition to adjust the location
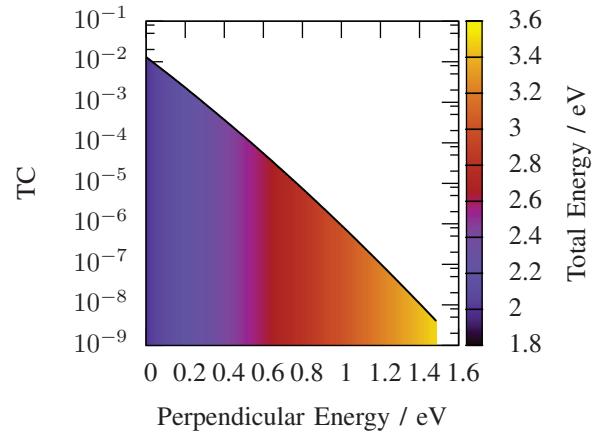

Fig. 3.   Tunneling probability as a function of perpendicular energy $E_\perp$ for the piece-wise linear band diagram described in Fig. 6

of this transition [2]. In order to satisfy conservation of momentum, total and perpendicular components of momentum are matched. From (7), the transmission coefficient (TC) can be written in terms of total momentum and perpendicular
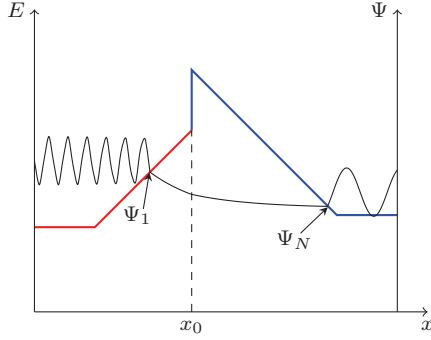
Fig. 4.   TC calculation through the tunneling barrier using QTBM

Fig. 5.   Effect of considering both valence and conduction components to the barrier

momentum. Total momentum from the valence band must equal the momentum in the conduction band. By matching the momentum in the valence band $(k_{\mathrm{v}}(x_0))$, with the momentum in the conduction band $(k_{\mathrm{c}}(x_0))$ the transition location (x_0) is obtained,

$$m_{\mathrm{v}}(E - E_{\mathrm{v}}(x_0)) = m_{\mathrm{c}}(E_{\mathrm{c}}(x_0) - E). \qquad (8)$$

Perpendicular momentum of a carrier in the valence band $(k_{\mathrm{v}\perp})$ must equal the perpendicular momentum in the conduction band, $(k_{\mathrm{c}\perp})$

$$m_{\mathrm{v}\perp}^* E_{\mathrm{v}\perp} = m_{\mathrm{c}\perp}^* E_{\mathrm{c}\perp}. \qquad (9)$$

This condition is employed in order to compute the energy barrier increase due to the perpendicular component of the band-to-band tunneling, as shown in Fig. 2(e).

B. TC Calculation

Computation of current requires a computation of the transmission coefficient. Recently, the Wentzel-Kramers-Brillouin (WKB) approximation has been used for this task [2]. The analytical WKB method can easily be applied to triangular barriers. In order to improve accuracy of the TC calculation, the quantum transmitting boundary method (QTBM) is implemented for this work. QTBM is numerically stable, efficient and flexible [4]. In this work, we have used this method to compute the band-to-band tunneling in direct semiconductors. Our approach allows for a seamless implementation of parameter changes between the two energy bands: arbitrary barrier shape and the effective mass transition. The energy barrier in the band gap is described as valence band-like until the transition point and conduction band-like after the transition point, allowing for a simple barrier to be extracted. In the QTBM approach, this simply requires a transition of parameters, such as energy in the barrier $E(x)$ and effective mass m^*. Computation of the transmission coefficient is then performed by calculating the wave function through the barrier, Fig. 4. Ψ_1 represents the wave function at the entry point to the barrier and Ψ_{N} is the final wave state after tunneling,

$$\Psi_1(x) = A_1 e^{ik_1 x} \qquad (10a)$$

$$\Psi_{\mathrm{N}}(x) = A_N e^{ik_{\mathrm{N}} x}. \qquad (10b)$$
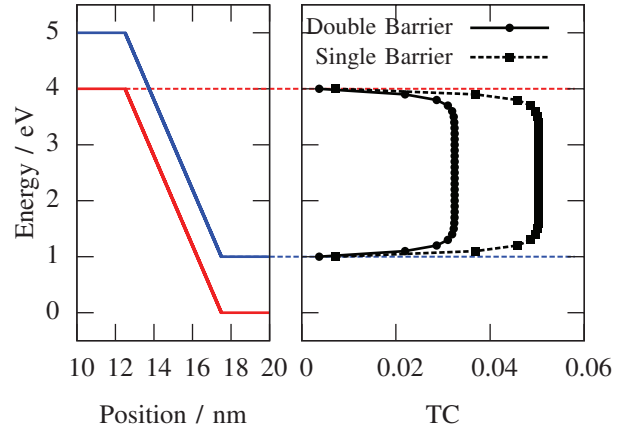
QTBM computes the transmission coefficient from the wave amplitudes,

$$TC = \frac{k_1 m_1}{k_{\mathrm{N}} m_{\mathrm{N}}} \frac{|A_{\mathrm{N}}|^2}{|A_1|^2}. \qquad (11)$$

In this work, we have implemented a one-dimensional model based on the QTBM method to compute the inter-band tunneling TC, as part of the Vienna Schrödinger Poisson (VSP) solver framework [5].

III. RESULTS

In order to validate our model, transmission coefficient and current calculations are performed for a range of conditions.

A. Barrier Change Effects

As shown in Fig. 1, this work implements a modification to the barrier between valence and conduction bands to consider influences of both regions. This allows for the consideration of effective mass and barrier potential transition from valence band to conduction band properties. Simple, single-triangular energy bands are simulated, along with the presented model, in order to demonstrate the effect of this energy barrier change. From Fig. 5, a significant difference in TC can be observed. The single-triangular barrier result shows a larger transmission coefficient than the double-triangular barrier. This over-estimation in the single-triangular barrier approach can be explained by the absence of valence band parameter consideration. Effective mass of the carrier in the valence band portion of the barrier is much larger, reducing the transmission coefficient. This effect is clearly observed in the double-triangular barrier simulation.

B. InAs Junction

In order to validate our model, TC is computed for a triangular barrier as well as for a highly doped InAs p-n junction. The energy bands and resulting TC for the triangular barrier are shown in Fig. 6. The flexibility of the QTBM implementation allows us to use arbitrary energy band shapes. To
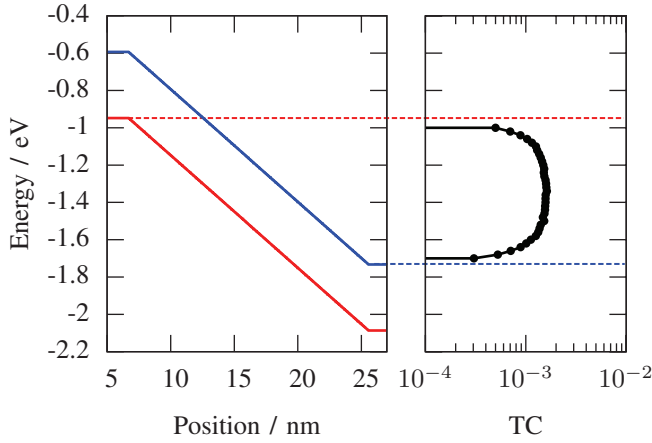
Fig. 6. Band diagram and the computed transmission coefficient for piece-wise linear energy bands
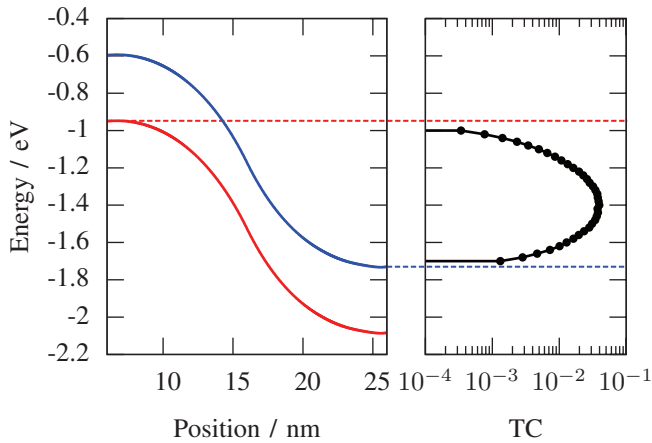

Fig. 7. Tunneling current density of a highly doped InAs p-n junction from Fig. 8

Fig. 8. Band diagram and the computed transmission coefficient for a highly doped InAs p-n junction

Fig. 9. Tunneling current density for different symmetric ($N_D = N_A$) doping levels of an InAs p-n junction

demonstrate this, TC is computed for a highly doped InAs p-n junction ($N_D=N_A=3 \times 10^{19} \mathrm{cm}^{-3}$). Using a self-consistent Schrödinger-Poisson loop, we computed the conduction and valence energy bands. These are then used to obtain the TC, shown in Fig. 8. The highly doped InAs p-n junction was used to simulate the tunneling current in Fig. 7. A range of doping values was studied for the junction in order to examine the effect of doping on the tunneling current. These results are shown in Fig. 9.

IV. CONCLUSION

Using the developed model, we are able to simulate transmission coefficients and current for band-to-band tunneling in direct semiconductors with increased flexibility and improved accuracy. The single-triangular barrier was shown to overestimate the transmission coefficient, and simplifying the energy barriers to triangular-shaped results in further computation inaccuracies. By combining the double-triangular tunneling barrier and QTBM, we propose an accurate and numerically stable method to compute band-to-band tunneling current.
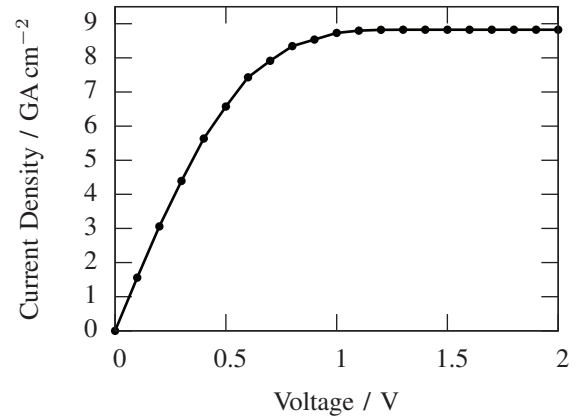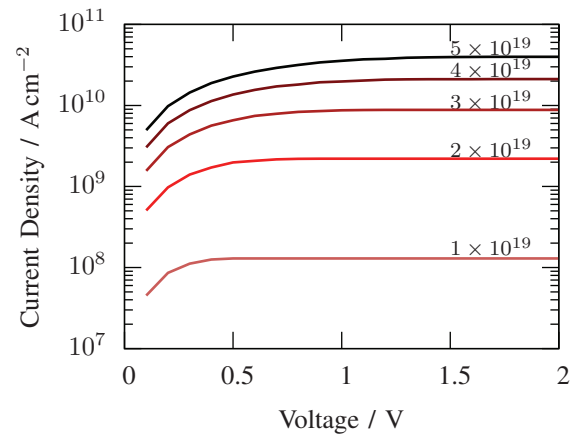
REFERENCES

[1] S. Sze and K. K. Ng, *Physics of Semiconductor Devices*. John Wiley & Sons, Inc., 2007.
[2] J. T. Teherani, "Band-to-Band Tunneling in Silicon Diodes and Tunnel Transistors," Master of Science in Electrical Engineering and Computer Science, Massachusetts Institute of Technology, June 2010.
[3] D. Sarkar and K. Banerjee, "Metallic-nanoparticle assisted enhanced band-to-band tunneling current," *Appl. Phys. Lett.*, vol. 99, p. 133116, 2011.
[4] C. S. Lent and D. J. Kirkner, "The quantum transmitting boundary method," *Journal of Applied Physics*, vol. 67, p. 6353, 1990. [Online]. Available: http://dx.doi.org/10.1063/1.345156
[5] M. Karner, A. Gehring, S. Holzer, M. Pourfath, M. Wagner, W. Goes, M. Vasicek, O. Baumgartner, C. Kernstock, K. Schnass, G. Zeiler, T. Grasser, H. Kosina, and S. Selberherr, "A multipurpose Schrödinger-Poisson Solver for TCAD applications," *Journal of Computational Electronics*, vol. 6, pp. 179–182, 2007. [Online]. Available: http://dx.doi.org/10.1007/s10825-006-0077-7